



HAL
open science

Optical methods to investigate the enhancement factor of an oxygen-sensitive colorimetric reaction using microreactors

Lixia Yang, Nicolas Dietrich, Karine Loubiere, Christophe Gourdon, Gilles Hébrard

► **To cite this version:**

Lixia Yang, Nicolas Dietrich, Karine Loubiere, Christophe Gourdon, Gilles Hébrard. Optical methods to investigate the enhancement factor of an oxygen-sensitive colorimetric reaction using microreactors. *AICHE Journal*, 2016, vol. 63 (n° 6), 13 p. 10.1002/aic.15547 . hal-01601916

HAL Id: hal-01601916

<https://hal.science/hal-01601916>

Submitted on 18 Jan 2018

HAL is a multi-disciplinary open access archive for the deposit and dissemination of scientific research documents, whether they are published or not. The documents may come from teaching and research institutions in France or abroad, or from public or private research centers.

L'archive ouverte pluridisciplinaire **HAL**, est destinée au dépôt et à la diffusion de documents scientifiques de niveau recherche, publiés ou non, émanant des établissements d'enseignement et de recherche français ou étrangers, des laboratoires publics ou privés.



Open Archive TOULOUSE Archive Ouverte (OATAO)

OATAO is an open access repository that collects the work of Toulouse researchers and makes it freely available over the web where possible.

This is an author-deposited version published in : <http://oatao.univ-toulouse.fr/>
Eprints ID : 19306

To link to this article : DOI : 10.1002/aic.15547
URL : <https://doi.org/10.1002/aic.15547>

To cite this version :

Yang, Lixia and Dietrich, Nicolas and Loubiere, Karine and Gourdon, Christophe and Hebrard, Gilles *Optical methods to investigate the enhancement factor of an oxygen-sensitive colorimetric reaction using microreactors*. (2017) *AIChE Journal*, vol. 63 (n° 6). pp. 2272-2284. ISSN 0001-1541

Any correspondence concerning this service should be sent to the repository administrator: staff-oatao@listes-diff.inp-toulouse.fr

OPTICAL METHODS TO INVESTIGATE THE ENHANCEMENT FACTOR OF AN OXYGEN-SENSITIVE COLORIMETRIC REACTION USING MICROREACTORS

Lixia Yang^{a,b,c}, Nicolas Dietrich^{a,c*}, Karine Loubière^{b,c}, Christophe Gourdon^{b,c}, Gilles Hébrard^{a,c}

a Laboratoire d'Ingénierie des Systèmes Biologiques et des Procédés (LISBP), Université de Toulouse, CNRS, INRA, INSA, Toulouse, France

b Laboratoire de Génie Chimique LGC, Université de Toulouse, CNRS, INPT, UPS, Toulouse, France

c Fédération de Recherche FERMAT, CNRS, Toulouse, F-31400 Toulouse, France

Abstract: Visualization of mass transfer is a powerful tool to improve understanding of local phenomenon. The use of an oxygen-sensitive dye (colorimetric technique¹) has showed its relevancy for locally visualizing and characterizing gas-liquid mass transfer at different scales^{2,3}. At present, the occurrence of a possible enhancement of the gas-liquid mass transfer by this reaction has not been yet demonstrated. This paper aims at filling this gap by evaluating the Hatta number Ha and the enhancement factor E associated with the oxygen colorimetric reaction when implementing in milli/micro channels. For that, as data on the kinetic of the colorimetric reaction are seldom in the literature, the reaction characteristic time was firstly estimated by carrying out experiments in a microchannel equipped with a micromixer. The diffusion coefficients of dihydroresorufin and O_2 were then determined by implementing two original optical methods in a specific coflow microchannel device, coupled with theoretical modelling. The knowledge of these parameters enabled at last to demonstrate that no enhancement of the gas-liquid mass transfer by this colorimetric reaction existed. Complementary information about the reliability of the colorimetric technique to characterize the gas-liquid mass transfer in milli/micro systems was also given.

Keywords: gas-liquid mass transfer, kinetic of an oxygen colorimetric reaction, enhancement factor, milli/micro reactor, diffusion coefficient

Introduction

Due to various advantages (controlled flow structure, high surface-to-volume ratio and enhanced heat and mass transfer), microstructured technologies have received more and more attentions as being promising process intensification technologies enabling to carry out chemical reactions under controlled and safe conditions with high yield and selectivity. Gas/liquid reactions play an important role in scientific research and industrial application fields dealing with flow chemistry: for example one can cite oxidation^{4,5}, catalytic hydrogenation⁶ and photocatalytic oxidation^{7,8}. When implementing such reactions, it is essential to perfectly characterize and control the mass transfer between both phases insofar as, depending on the chemical kinetics, it can become the limiting step and thus induce a decrease of the reaction performances.

Recently, the investigation of gas-liquid mass transfer in microreactors has been the subject of a growing literature^{9,10,11,12,13}. Roudet et al.⁷ proposed an original method to characterize the benefits of a meandering geometry with respect to straight channels; for that, the dissolved oxygen concentrations were measured, by using micro sensors, at different locations along the channel length and, thanks to a modelling approach, the overall volumetric gas-liquid mass transfer coefficients were accurately determined. Mikaelian et al.¹¹ established a model to describe the dissolution of a chain of spherical pure gas bubbles into a non-volatile liquid along square and circular microchannels. Amongst these works, the gas-liquid mass transfer characteristics were classically measured by analyzing the solute concentration of samples collected at the inlet and outlet of microreactors, or the time-dependent variations of the bubble sizes^{10,12}. The latter methods might lead to an inaccurate characterization as the sample collection and phase separation times are not usually taken into account. In addition, they do not enable to distinguish the contributions to mass transfer of the bubble formation, bubble flow and phase-separation as no local information of the gas-liquid mass transfer is acquired. To overcome these limitations, it is therefore necessary to implement online and local approach. In this perspective, Dietrich

et al.¹ proposed a colorimetric technique, based on the use of an oxygen-sensitive dye, to locally visualize and characterize the gas-liquid mass transfer associated with bubbles flowing in a millimetric square channel. The oxygen-sensitive dye used was resazurin which is a phenoxazin-3-one dye widely used for testing bacterial or yeast contamination in biological fluids and milk, and also identifying the semen quality by colorimetry since 1950s^{13,14}. Afterwards, this technique has been successfully implemented in other geometries^{2,3}, thus demonstrating its reliability to characterize the oxygen mass transfer and to elucidate the complex mechanism of gas-liquid mass transfer. Nevertheless, it should be pointed out that the kinetics data about the colorimetric reaction between oxygen and dihydroresorufin remain rare¹⁵ and that the occurrence of a possible enhancement of the gas-liquid mass transfer by this reaction has not been rigorously demonstrated. Dietrich et al.¹ has admittedly showed that the liquid-side mass transfer coefficients obtained by this method and the ones measured by oxygen microsensors were identical, but any enhancement factor was calculated. This lack of knowledge necessitates an in-depth characterization of this oxygen-sensitive colorimetric reaction, with the aim of better defining the conditions required to implement accurately this colorimetric technique.

With this in mind, the objective of the present study is to rigorously determine the enhancement factor E associated with the oxygen-sensitive colorimetric reaction when implementing in micro/millichannels. For that, the knowledge of the kinetics of the reaction and of the diffusion coefficients of both oxygen and dihydroresorufin into the liquid under test, is a prerequisite. As these parameters are unknown, original methods will be proposed to determine them: they will be based on specific experiments in microfluidic devices, coupled with modeling approaches. The paper will be composed of four main sections. The first section will remind the knowledge available on the kinetics of the colorimetric reaction and the theoretical background associated with the enhancement factor concept. Section “Material and methods” will be mainly devoted to the description of the three experimental set-up designed for measuring on the one hand the reaction characteristic time (experiments in a

microchannel equipped by a micromixer) and on the other hand, the diffusivity coefficients of dihydroresorufin and O₂ (optical methods in a specific coflow microchannel device). Section “Modeling methods” will focus on the modelling methods used to analyze the experimental data so as to access the diffusion coefficients of dihydroresorufin and O₂. The results will be presented and discussed in Section “Results and discussion”: they will concern the reaction characteristic time, the diffusion coefficients and the calculation of the Hatta number and the enhancement factor ; such findings will at last enable to identify the conditions whether the colorimetric reaction can enhance the oxygen mass transfer.

Background

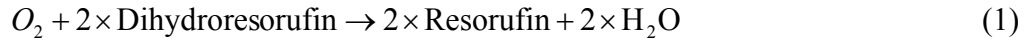
This section will describe firstly the data at present available on the kinetics of the colorimetric reaction and secondly the theoretical background associated to the enhancement factor concept, especially in the case of fast gas-liquid reactions. In a last time, the basic conditions required to experimentally acquire the characteristic time of gas-liquid reactions will be reminded as well as a brief state-of-art about the various optical methods existing to measure diffusion coefficients.

About the kinetics of the colorimetric reaction

The colorimetric technique proposed by Dietrich et al.¹ is based on the use of an oxygen-sensitive dye (resazurin, noted as R) which can react with oxygen in the presence of sodium hydroxide and glucose. In the reduced form, named dihydroresorufin (noted as B), the solution is colorless, while in presence of oxygen, the oxidized form, named resorufin (noted as C), is characterized by an intense pink color. The reaction scheme is reminded in Fig. 1. As shown by previous works^{1,3}, one of the main interest of this technique is that the extent of the oxidation reaction and so the amount of transferred (or dissolved) oxygen, are directly proportional to the color intensity (grey value), for a given concentration of resazurin. To make possible the visualization and the post-treatment of the colored fields in a given geometry, an optimal composition of the sodium hydroxide and glucose solution should be determined.

It results from a balance between the reaction kinetic rates and the requirement in terms of adequate color intensity levels: indeed, the kinetics for the oxidation reaction ($B + O_2 \rightarrow C$) should be quasi-instantaneous whereas the kinetics of the back reaction ($C \rightarrow B$) should be slow (few minutes).

In the present study, one focuses on the colorimetric reaction between dihydroresorufin (B) and oxygen (O_2):



(colorless) (pink)

Based on the literature background^{15,16}, one can assume that this colorimetric reaction is of a global order 2, with respect to the oxygen and to the dihydroresorufin. The rate of consumption of dihydroresorufin, r_B (or the rate of consumption of oxygen r_{O_2}) is then expressed as:

$$r_B = -\nu \cdot k_2 \cdot C_{O_2} \cdot C_B = \nu \cdot r_{O_2} \quad (2)$$

where k_2 is the reaction rate constant ($m^3 \cdot mol^{-1} \cdot s^{-1}$) and ν the stoichiometric coefficient equal to 2.

Theoretical considerations on Hatta number and enhancement factor

In presence of a chemical reaction, the mass flux of oxygen φ_{O_2} transferred from the gas phase to the liquid phase is expressed, as below:

$$\varphi_{O_2} = k_L \cdot a \cdot E \cdot (C_{O_2}^* - C_{O_2}) \quad (3)$$

where k_L is the liquid-side mass transfer coefficient ($m \cdot s^{-1}$), a the interfacial area (m^{-1}); $C_{O_2}^*$ the dissolved oxygen concentration at saturation ($kg \cdot m^{-3}$), and E the enhancement factor (-). The latter is defined by the ratio between the average fluxes of absorption with reaction and without reaction, thus it represents in a way the effect of “pumping” by the chemical reaction.

To determine E , the mass balances in the liquid film for both oxygen and dihydroresorufin (B) should be written¹⁹, using the expression of the second-order reaction kinetics (Eq. 2). It leads to:

$$-r_{O_2} = D_{O_2} \cdot \frac{d^2 C_{O_2}}{dy^2} = k_2 \cdot C_{O_2} \cdot C_B \quad (4)$$

$$-r_B = D_B \cdot \frac{d^2 C_B}{dy^2} = \nu \cdot k_2 \cdot C_{O_2} \cdot C_B \quad (5)$$

where D_{O_2} and D_B are the diffusion coefficient of O_2 and B respectively ($m^2 \cdot s^{-1}$), C_{O_2} and C_B the concentrations of O_2 and B at a given location y in the film respectively ($mol \cdot m^{-3}$); y the distance from the gas-liquid interface to the bulk liquid phase (m), where none convection and accumulation is assumed to occur.

The associated boundary conditions are:

- at the interface ($y = 0$): $C_{O_2} = C_{O_2}^*$ and $\frac{dC_B}{dy} = 0$ (B: non-volatile) (6)

- at the limit of the film ($y = \delta$), δ being the film thickness, the concentrations of both O_2 and B are the ones in the liquid bulk, which depend on the hydrodynamics of the reactor and on the transport phenomena through the liquid film. By assuming that the liquid bulk can be considered as perfectly mixed and that the liquid does not contain any dissolved oxygen, the boundary conditions are given by the mass balances in the liquid bulk when considering the chemical reaction and the fluxes transferred from the film by diffusion only towards the liquid bulk:

$$-D_{O_2} \cdot S \cdot \left(\frac{dC_{O_2}}{dy}\right)_{y=\delta} = Q \cdot C_{O_{2b}} + V_L \cdot r_{O_2} \quad (7)$$

$$-D_B \cdot S \cdot \left(\frac{dC_B}{dy}\right)_{y=\delta} = Q \cdot (C_{Bb} - C_{Bi}) + V_L \cdot r_B \quad (8)$$

where S is the gas-liquid interfacial area (m^2), Q the volumetric flow rate of the liquid dye solution ($m^3 \cdot s^{-1}$), V_L the liquid volume (m^3), $C_{O_{2b}}$ the concentration of O_2 in the liquid bulk, C_{Bi} and C_{Bb} the concentrations of B at the inlet of the reactor and in the liquid bulk respectively ($mol \cdot m^{-3}$).

By making these equations dimensionless, one can demonstrate that the concentration profiles, the absorption flux of oxygen and thus the enhancement factor depend on the following dimensionless numbers: the Hatta number Ha , the parameter Z , the Damköhler number Da and the parameter R , defined as below:

$$Ha^2 = \frac{k_2 \cdot C_{O_2}^* \cdot C_{Bb} \cdot \delta}{D_{O_2} \cdot \frac{C_{O_2}^* - 0}{\delta}} = \frac{k_2 \cdot C_{Bb} \cdot \delta^2}{D_{O_2}} = \frac{k_2 \cdot C_{Bb} \cdot D_{O_2}}{k_L^2} \quad (9)$$

$$Z = \frac{D_B \cdot C_{Bb}}{\nu \cdot D_{O_2} \cdot C_{O_2}^*} \quad (10)$$

$$Da = k_L \cdot a \cdot \tau = k_L \cdot a \cdot \frac{V_R}{Q} \quad (11)$$

$$R = \frac{k_2 \cdot C_{O_2}^* \cdot C_{Bb} \cdot \varepsilon_L}{k_L \cdot a \cdot C_{O_2}^*} = \frac{k_2 \cdot C_{Bb} \cdot \varepsilon_L}{k_L \cdot a} \quad (12)$$

The Hatta number Ha represents the ratio between the maximal rate of reaction in the liquid film and the mass flux crossing the film by diffusion; the parameter Z contains the ratio between the diffusion coefficients; the Damköhler number Da (also called the Number of Transfer Units) represents the ratio between the residence time and the characteristic time of gas-liquid mass transfer; R compares the maximum reaction rate of O_2 that can be achieved within the liquid with the maximum O_2 physical absorption rate, and ε_L the liquid hold-up.

In the case of a fast reaction regime in the diffusional film, for which Ha is higher than 3, Van Krevelen and Hoftijzer¹⁹ have shown that the enhancement factor becomes only a function of Ha and of the enhancement factor for instantaneous regime (also called the limit enhancement factor), noted E_i and defined as:

$$E_i = 1 + Z = 1 + \frac{D_B \cdot C_{Bb}}{\nu \cdot D_{O_2} \cdot C_{O_2}^*} \quad (13)$$

In this case, these authors proposed the following approximated solution for the enhancement factor E :

$$E = \frac{Ha \cdot \sqrt{\frac{E_i - E}{E_i - 1}}}{\tanh(Ha \cdot \sqrt{\frac{E_i - E}{E_i - 1}})} \quad (14)$$

The latter developments reveal that the calculation of the enhancement factor requires the knowledge of the kinetics constant k_2 , and of both diffusion coefficients, D_{O_2} and D_B . As these parameters are unknown in the present case, the following two subsections will present some theoretical considerations that need to be taken into account for determining a reaction characteristic time and a brief state-of-art about the methods for measuring diffusion coefficients respectively.

Conditions required to determine the characteristic time of gas-liquid reactions

When carrying out a gas-liquid reaction, two distinct phenomena simultaneously exist in a given experimental device: the transfer of the reactant from the gas phase to the liquid phase and the reaction itself that can occur in the liquid film, in the liquid bulk or in both locations. For experimentally determining the associated reaction characteristic time, it is essential to firstly eliminate the influence of the gas-liquid mass transfer. For that, one of the most commonly used method consists in previously dissolving the reactant contained in the gas phase in the solvent present in the other phase^{20,21}.

To use it as a method to characterize gas-liquid mass transfer, the colorimetric reaction between dihydroresorufin (B) and oxygen must be fast^{1,3}, thus making quite difficult the acquisition of the associated kinetic parameters, in particular in conventional batch reactors. Indeed, such technologies do not often guarantee that the time required by the reagents to be perfectly mixed (mixing time, t_m) is sufficiently shorter than the reaction characteristic time (t_r), here typically below 1s. Recently, the use of

micromixers in microfluidic devices has been proven to be an interesting solution for kinetic data acquisition, as overcoming the conventional mixing limitations^{22,23,23}.

Consequently, in the present study, it has been thus chosen to carry out the fast colorimetric reaction between oxygen and dihydroresorufin solution in a microchannel equipped with a micromixer. In addition, the experiments will be performed by using deionized water previously saturated with O₂ to avoid any gas-liquid mass transfer limitations. The associated experimental set-up will be described in the section “Material and methods”, in the sub-section “Experimental set-up for measuring the reaction characteristic time”.

Brief state-of-art about the optical methods for measuring diffusion coefficients

Due to their advantages, such as quick response, real-time analysis of regions, non-invasive and high-resolution, the optical methods have been widely developed to study the diffusion process since the pioneering work of Hauf²⁵. Qualitative and quantitative data could be acquired by optical methods, and then compared with analytical or numerical investigations in order to develop more complete phenomenological models for the diffusive mechanisms²⁶. Traditional optical approaches such as Taylor’s method²⁷ has been commonly developed and employed to measure diffusion coefficients in liquids. The principle of Taylor’s method is to inject a sharp pulse of solute into a slow and steady laminar flow of solvent in a tube of circular section and suitable length; the solute then flows with the mean velocity of the solvent flow and shows much pronounced axial dispersion by the combined action of the parabolic solvent velocity profile and the radial molecular diffusion. The main limitation of this method is to require relatively long capillary and so long time experiments (several hours). In the last decade, the development of lasers and electronic cameras has enabled to make a considerable progress in the development of new optical measurement techniques, for example holographic interferometry²⁸,

speckle technique²⁹ and planar laser-induced fluorescence (PLIF) system³⁰. Such laser-based methods have the same common limitations, such as requirement of specific light source, and not easy to conduct.

In the present study, an original optical technique will be proposed to measure the diffusion coefficients. It is based on the laminar diffusion of molecules in a coflow microfluidic device and on the visualization of the change of colors occurring when the diffusion and the colorimetric reaction take place. The main advantages of this method are to avoid the use of laser and to be less time-consuming compared with conventional optical approaches. The experimental set-up for implementing the technique will be described in the section “Material and methods”.

Material and methods

As highlighted in Section “Background”, three parameters have to be determined to calculate the Hatta number Ha and the enhancement factor E associated with the O_2 colorimetric reaction: the kinetics constant k_2 , and both diffusion coefficients of dihydroresorufin and O_2 , D_B and D_{O_2} . In this section, the three experimental set-ups used to determine these parameters will be described as well as the operating conditions and the image acquisition and post-treatment methods implemented.

Fluid properties

All the experiments were performed at 293.15 K and atmospheric pressure. The dye solution consisted of D-glucose anhydrous (Fischer Scientific[®], CAS 50-99-7), sodium hydroxide (VWR[®], CAS 1310-73-2), both diluted at 20 g·L⁻¹ in deionized water (conductivity: 51.2 μS·m⁻¹), and resazurin (Sigma Aldrich[®], CAS 62758-13-8, molecular mass: 229.19 g·mol⁻¹) which concentration was fixed at 0.117 g L⁻¹ (5.10×10⁻⁴ mol·L⁻¹). The concentration of resazurin was chosen with respect to the reaction stoichiometry and to the oxygen concentration at saturation $C_{O_2}^*$ in the reactional medium. The

density ρ_L , dynamic viscosity μ_L and static surface tension σ_L were measured by means of a pycnometer ($\rho_L \pm 0.2 \text{ kg}\cdot\text{m}^{-3}$), a RM180 Rheomat Rheometric Scientific[®] viscometer ($\mu_L \pm 10^{-3} \text{ mPa}\cdot\text{s}$), and a Digidrop GBX[®] or Krüss tensiometer ($\sigma_L \pm 0.5 \text{ mN}\cdot\text{m}^{-1}$) respectively. The oxygen saturation concentration $C_{O_2}^*$, was measured by implementing the Winkler technique³¹ and by means of optical oxygen probes (Hach-Lange[®]). All the physicochemical properties are reported in Table 1.

Experimental set-up for measuring the reaction characteristic time

The experimental set-up implemented to measure the reaction characteristic time is illustrated in Fig. 2. It consisted of a microfluidic device composed by a transparent PTFE tube (inner diameter $d = 1 \text{ mm}$) fixed at the outlet of a micromixer. The SIMM-V2 micromixer (Slit Interdigital Micromixer, IMM Germany) was chosen to efficiently mix the two liquid phases. The cross-sectional area of its standard mixing channel A was $45 \times 200 \text{ }\mu\text{m}^2$ and its inner volume V_m was $8 \text{ }\mu\text{L}$. Two high pressure syringe pumps (neMESYS high pressure syringe pump module, highest pressure up to 510 bar, Cetoni[®] GmbH, Germany) were used to deliver the deionized water saturated with O_2 and the dye solution from two 20 mL syringes, each connected to the micromixer by a transparent PTFE tube (inner diameter $d = 1 \text{ mm}$). The dye solution (B) was previously flushed with nitrogen and was thus colorless when entering in the micromixer. The volumetric flow rates of these two liquid phases (Q_W : deionized water saturated with O_2 ; Q_R : dye solution) were identical in all the experiments, which both ranged from 80 to 2000 $\text{mL}\cdot\text{h}^{-1}$. The associated liquid velocities inside the micromixer were defined by

$$u = (Q_W + Q_R) / A \quad (15)$$

They varied from 4.94 to 123.46 $\text{m}\cdot\text{s}^{-1}$, and the corresponding Reynolds number Re ($= \rho_L \cdot d_h \cdot u / \mu_L$, d_h : hydraulic diameter of the micromixer, m) from 326 to 8152. A LED light source

(Rosco[®], LitePad HO90) and a camera (dnt[®], DigiMicro 2.0 Scale) were set at the outlet of the micromixer to acquire images of the solution leaving the micromixer.

Experimental set-up for the measuring the diffusion coefficient of dihydroresorufin D_B

Since dihydroresorufin (noted as B) is colorless, it is impossible to visualize it experimentally, whereas for the pink resorufin (noted as C), it is possible. Note that the molecular formula of dihydroresorufin being quite similar to that of resorufin apart from the hydrogen ion (see in Fig. 1), it can hereafter be assumed that the diffusion coefficient of dihydroresorufin D_B is equal to the one of resorufin D_C .

The experimental set-up for measuring D_B was based on the concept of the two-liquid phase quasi-steady laminar coflow dispersion^{32,33}. A T-junction 3 way connector was used to generate the laminar coflow. The experimental set-up is illustrated in Fig. 3 (a) and (b). The dye solution (previously saturated with O₂ to make sure that all the dihydroresorufin was converted to pink resorufin) and deionized water saturated with O₂ were delivered from a 60 mL syringe by syringe pumps III and IV (Harvard Apparatus, PHD 22/2000, USA) respectively. The connections to the two inlets of the T-junction connector were different for each solution: a capillary (inner diameter $d_{c,in} = 250 \mu\text{m}$, outer diameter $d_{c,out} = 365 \mu\text{m}$, cross-sectional area $A' = \pi \cdot d_{c,in}^2 / 4 = 4.91 \times 10^{-8} \text{m}^2$), and a transparent PTFE tube (inner diameter $d_{t,in} = 1 \text{mm}$, outer diameter $d_{t,out} = 3 \text{mm}$). At the outlet of the connector, the capillary was carefully inserted and aligned to the central axis of the tube. Such experimental set-up made possible to generate two-liquid phase laminar coflows under appropriate operating conditions. The dye solution was injected from the capillary and the deionized water saturated with O₂ from the PTFE tube, which meant that the flow of the dye solution was surrounded symmetrically and annularly by the deionized water at the outlet tube of the connector (see Fig. 3. b). The same camera as in the

micromixer experiments was set at the outlet of the connector to record the radial profiles of pink color intensity and their evolution along the axial position in the PTFE tube.

The volumetric flow rates of these two liquid phases (Q_w' for deionized water saturated in oxygen; Q_R' for dye solution) were both ranged from 3 to 12 mL·h⁻¹. The associated liquid velocities u' ($= Q_R' / A'$) inside the capillary were ranged between 0.017 m·s⁻¹ and 0.068 m·s⁻¹, the capillary numbers Ca' ($= \mu_L \cdot u' / \sigma_L$) from 2.53×10^{-4} to 1.01×10^{-3} , and the Reynolds numbers Re' ($= \rho_L \cdot d_h' \cdot u' / \mu_L$, d_h' : hydraulic diameter of the capillary, m) from 4.2 to 16.9.

Experimental set-up for measuring the diffusion coefficient of oxygen D_{O_2}

The experimental set-up to measure D_{O_2} was identical to the one described to measure D_B , except that the deionized water saturated with O₂ was injected from the capillary and the dye solution (previously flushed by nitrogen, colorless dihydroresorufin) from the tube. As a consequence, in this case, the flow of deionized water was surrounded symmetrically and annularly by the dye solution at the outlet tube of the connector. Both volumetric flow rates ranged from 3 to 12 mL·h⁻¹. The associated liquid velocities u'' inside the capillary were defined as $0.017 \text{ m} \cdot \text{s}^{-1} \leq u'' = Q_w'' / A' \leq 0.068 \text{ m} \cdot \text{s}^{-1}$, and the Reynolds numbers Re'' ($= \rho_{L,w} \cdot d_h' \cdot u'' / \mu_L$) ranged from 4.2 to 16.9.

Image acquisition and post-treatment

For all the experiments, the digital micro camera (dnt[®], DigiMicro 2.0 Scale) was used to record the images after the establishment of the steady state (around 15 min). The acquired images were colorful. In a first step, a background image was subtracted from the raw images to eliminate the eventual effect of a non- uniform distribution of backlight. The images were then converted to greyscale images using

Matlab (R2011b) software, thus enabling to extract a grey value (noted as GV) for each pixel of the image. Due to the established linear relationship between GV and the extent of the colorimetric reaction for a given concentration of resazurin (i.e. the amount of the reacted oxygen)^{1,3}, these grey values GV measured were directly proportional to the concentrations of dihydroresorufin or to the equivalent concentration of dissolved oxygen. Note that in this study, as being not necessary, the calibration curve enabling to transform GV to the corresponding equivalent concentration of O_2 (i.e. calculation of the linear proportionality coefficient) was not determined.

For the micromixer experiment, an average grey value, noted as \overline{GV} , was calculated by averaging the grey values GV at each pixel of the image taken at the outlet of the micromixer under each operating condition. Almost ten images were used to calculate \overline{GV} .

For the experiments related to the measurement of the diffusion coefficient of D_B , a typical image is displayed in Fig. 4 (a). It was decided to choose the origin of the radial r -axis at the midline of the capillary and the origin of the axial z axis at the outlet of the capillary. By image treatment, the grey value of each pixel along the r -direction at a given axial position z , noted as $GV(r, z)$, could be extracted. From this, the maximum grey value, noted as $GV_{\max}(r, z)$, associated to a given radial profile could be obtained. The value of $GV_{\max}(r, z)$ was found to be unchanged at various z , and was then noted GV_{\max} . The grey value of the background image was noted $GV_0(r, z)$. At last, $GV(r, z)$ was normalized using GV_{\max} and $GV_0(r, z)$, leading to define GV^* such as $GV^* = (GV(r, z) - GV_0(r, z)) / (GV_{\max} - GV_0(r, z))$. The radial location r was also normalized by the diameter of the tube, noted as r^* .

The evolution of the normalized grey value GV^* (which are proportional to the normalized concentration of resorufin) as a function of the normalized radial position r^* is shown in Fig. 4 (b) for various axial positions z . It can be observed that:

- (i) in the central zone of the colored flow corresponding to radial positions r^* below 0.3, the normalized grey value remains almost unchanged (approximately to be 1) whatever the axial position. This value of 0.3 does not exactly correspond to the diameter of the inner capillary, 0.25 mm; this can be explained by the fact that for the high concentration zone, the color intensity is more sensitive to the concentration of the resorufin. Thus it is reasonable to have a higher $GV(r, z)$ (close to GV_{\max}) at the position near the outlet of the capillary.
- (ii) a high gradient area exists close to the edge of the colored flow, thus illustrating the occurrence of the diffusion process. It is precisely this high gradient area that will be used in the modelling section afterwards (see section “Diffusion coefficient of dihydroresorufin D_B in deionized water”).

For the experiments related to the measurement of the diffusion coefficient of D_{O_2} , the same method was employed to obtain the evolution of the normalized grey value GV^* versus the normalized radial position r^* .

Modeling methods

The diffusion coefficients of both dihydroresorufin and oxygen will be determined by identification of the experimental radial profiles of concentrations (grey values) with the theoretical ones.

To predict the concentration fields resulting from a purely diffusion mechanism, the classical diffusion equation based on a material balance should be considered. In cylindrical coordinates, it is written as³⁴:

$$\frac{\partial C}{\partial t} = D \cdot \left[\frac{1}{r} \cdot \frac{\partial}{\partial r} \left(r \cdot \frac{\partial C}{\partial r} \right) + \frac{1}{r^2} \cdot \frac{\partial^2 C}{\partial \theta^2} + \frac{\partial^2 C}{\partial z^2} \right] \quad (16)$$

where r, θ, z are the radial, angular and axial positions in the tube (m) depicted as in Fig. 4 (a); t the diffusion time (s) which is, using the equivalence time-space in the tube, equal to:

$$t = z / u' \quad (17)$$

Where u' is the mean velocity of the dye solution in the tube, $\text{m} \cdot \text{s}^{-1}$.

From Fig. 4 (a), it could be known that the pink zone after the outlet of the capillary presents the colored flow of resorufin by the pressure-driven flow at the capillary outlet. Due to the operations at low Reynolds numbers and low concentrations (convective mass transfer negligible), the two flows were considered as pure laminar, and the transport between them should be diffusive: along the r direction, there should exist only molecular diffusion. As a consequence, for the modelling, it was assumed that (i) the color intensity gradient only appears along the r -direction, (ii) the diffusion along r -direction was axisymmetric (independent of θ), and (iii) the diffusion along the z -direction is negligible. Eq. (16) was then reduced to:

$$\frac{\partial C}{\partial t} = D \cdot \left[\frac{1}{r} \cdot \frac{\partial}{\partial r} \left(r \cdot \frac{\partial C}{\partial r} \right) \right] = \frac{D}{r} \cdot \frac{\partial C}{\partial r} + D \cdot \frac{\partial^2 C}{\partial r^2} \quad (18)$$

In the conditions implemented in this paper, it can be shown that the first term $\frac{D}{r} \cdot \frac{\partial C}{\partial r}$ could be neglected. Eq. (18) was further reduced to:

$$\frac{\partial C}{\partial t} = D \cdot \frac{\partial^2 C}{\partial r^2} \quad (19)$$

Two methods were investigated to solve this equation, as presented below.

Markov Chain Monte Carlo (MCMC) method

Eq. (19) admits an analytical solution in the cases where the following of boundary and initial conditions are verified:

$$\begin{aligned} \text{Boundary condition 1:} & \quad C(r, t) = C_{max}(r, t) & \quad \text{at } r = d_{c,in}/2 \text{ and } t \geq 0 \\ \text{Boundary condition 2:} & \quad C(r, t) = C_0(r, t) & \quad \text{at } r = d_{t,in}/2 \text{ and } t \geq 0 \\ \text{Initial condition :} & \quad C(r, t) = 0 & \quad \text{at } t = 0 \text{ and } 0 \leq r \leq d_{t,in}/2 \end{aligned}$$

where $C_{max}(r, t)$ is the highest concentration (corresponding to the highest grey value, $GV_{max}(r, t)$), $C_0(r, t)$ is the initial concentration (corresponding to the grey value of the background image $GV_0(r, t)$).

Under these conditions, Eq. (19) admits the following analytical solution ³⁷:

$$\text{For } r > d_{c,in}/2 : \quad \frac{C(r, t) - C_0(r, t)}{C_{max}(r, t) - C_0(r, t)} = GV^* = 1 - erf\left[\frac{r}{2\sqrt{Dt}}\right] \quad (20)$$

where the error function $erf(\cdot)$ is defined as:

$$erf(u) = \frac{2}{\sqrt{\pi}} \cdot \int_0^u \exp(-\eta^2) \cdot d\eta \quad (21)$$

In a first step, a Markov Chain Monte Carlo (MCMC) method was implemented on Matlab[®] software in order to solve Eq. (19)³⁶ under the relevant initial and boundary conditions. The associated objective was to compare the experimental and theoretical concentration profiles at different times (i.e. z axial positions) and to efficiently optimize the different parameters in order to find the best fit between experimental and theoretical data.

For the measurement of the diffusion coefficient of dihydroresorufin D_b (see Fig. 3. b and Fig. 4. a), the calculation was firstly done by considering the radial profile of grey value obtained at an axial position close to the outlet of the capillary ($z = 0.2$ mm). It was then observed that the MCMC method provided a highly accurate estimation of the diffusive front (i.e. grey value displacement) with a very good agreement with experimental results (deviation less than 3%, results not shown here). However,

the predicted diffusion coefficient D_B , was found to be equal to $3 \times 10^{-6} \text{ m}^2 \cdot \text{s}^{-1}$, which is not at all the order of magnitude of the expected diffusion coefficient of macromolecules into liquids (10^{-11} to $10^{-10} \text{ m}^2 \cdot \text{s}^{-1}$ ^{25,42,38}). This result suggested that at the outlet of the capillary, (i.e. during the first stages of the diffusion process), some convective effects existed and were dominating over the diffusion process. As a consequence, Eq. (20) and the associated initial and boundary conditions could not be applied with the experimental conditions imposed. For these reasons, another method was implemented to solve Eq. (19) and fit accurately D_B .

Finite difference element scheme

In order to escape from the convective effects occurring at the outlet of the capillary, an alternative calculation method, the explicit FTCS (Forward-Time Central-Space) finite difference element scheme³⁹, was employed: it enabled to directly solve Eq. (19) without imposed initial conditions, but with using an experimental normalized concentration profile.

As the diffusion process could be considered with an instantaneous plane source (round) and in a semi-infinite medium, Eq. (19) was then reduced to³⁵:

$$\frac{\partial C}{\partial t} = D \cdot \left[\frac{\partial^2 C}{\partial x^2} + \frac{\partial^2 C}{\partial y^2} \right] \quad (22)$$

where $x = r \cdot \cos \theta$ and $y = r \cdot \sin \theta, 0 \leq \theta \leq 2\pi$.

The diffusion process was simulated in Matlab[®] (R2011b) software starting from an experimental concentration field associated with a time t_0 after a time t_1 under a given D . This time t_0 corresponded to the axial position z for which the edge of the colored flow began to be parallel to the wall of the tube. The resulted simulated profile was then compared to the corresponding experimental profile when diffusion time equal to $(t_0 + t_1)$.

It is important to note that for both the diffusions of dihydroresorufin and oxygen, the experimental profiles of grey values were in reality the result of the superposition of all the diffused amount of the molecule at each slice along r axis. As a consequence, it was necessary to sum up and then average all the concentration profiles predicted by the simulation (i.e. integration over all the radial positions) before comparison with the experimental profiles. Thus by changing the value of D , the simulated diffused results varied, and then the numerical results were compared with the experimental ones in order to determine the optimal D .

Results and discussion

Reaction characteristic time

Fig. 5 represents the variation of the average grey value \overline{GV} as a function of the residence time t_r inside the micromixer, the latter being calculated according to

$$t_r = \frac{V_m}{Q_t} = \frac{V_m}{Q_w + Q_R} \quad (23)$$

It can be observed that when $t_r > 130.9$ ms (at very small flow rates), a segregation phenomenon occurs, characterized by two distinct parallel flows corresponding to the deionized water saturated with oxygen (colorless) and the dye solution (pink). This phenomenon is due to the fact that the flow rates related to $t_r > 130.9$ ms are too small and below the minimum flow rate recommended by the supplier for using the micromixer. In these conditions, the micromixer is not able to mix efficiently both solutions.

When $t_r < 130.9$ ms, a plateau is reached, which indicates that the mixing is now efficient. The mixing time t_m associated with this kind of micromixer has been determined by Falk and Commenge⁴⁰: it is almost two orders of magnitude smaller than the residence time (0.04-0.68 ms compared to 7.2-180 ms). This shows that the ability to determine the kinetics of the colorimetric reaction by using this

microfluidic device will be imposed by the time t_r spent by the solution inside the micromixer. In other words, the color intensity fields observed at the outlet of the micromixer are related to the extent of the reaction at a time equal to t_r inside the micromixer, even if the fluids are in reality mixed in a significantly smaller time. For technical reasons (too high pressure drop), the minimum t_r that could be achieved in the present device is 7.2 ms, this value can be thus associated to a maximum value of the reaction characteristic time, noted $(t_{react})_{max}$, that is here experimentally accessible.

This value of $(t_{react})_{max}$ will be used later for the calculation of the Hatta number (see section “Hatta number Ha and enhancement factor E ”).

Diffusion coefficient of dihydroresorufin D_B in deionized water

As depicted in Fig. 4 (a), the edge of the colored flow is not parallel to the wall of the tube close to the outlet of the capillary due to the axial dispersion generated by some convective mechanisms along the r axis direction. Afterwards (i.e. at higher axial locations), the edge of the colored flow becomes parallel to the walls of the tube, thus meaning that the diffusion mechanism of resorufin from the inner flow to the surrounding one is purely radial. For this reason, the radial profile of normalized grey value (proportional to normalized concentration of resorufin) at $z = 2.2$ mm has been used as an initial condition in the explicit FTCS finite difference element scheme (corresponding to t_0) to simulate the dye concentration profile at $z = 2.6$ mm (corresponding to t_1). The best fitting between experimental and theoretical profiles has been obtained for $D_B = 2.25 \times 10^{-9} \text{ m}^2 \cdot \text{s}^{-1}$. The comparison between the predicted and experimental profiles at this axial position, is reported in Fig. 6 for $Q_R' = 3 \text{ mL} \cdot \text{h}^{-1}$, $Q_W' = 6 \text{ mL} \cdot \text{h}^{-1}$; a very good agreement is observed between these profiles. It can be noted that the optimization process has been performed considering the higher gradient area depicted in Fig. 4. (b), which corresponds to a purely radial diffusive mechanism.

To validate this value of D_B , this procedure has been repeated for several positions z (higher than 2.6 mm), using the experimental profile at the previous axial position for each one, and under two operating conditions ($Q_R' = 9 \text{ mL}\cdot\text{h}^{-1}$, $Q_W' = 9 \text{ mL}\cdot\text{h}^{-1}$) and ($Q_R' = 3 \text{ mL}\cdot\text{h}^{-1}$, $Q_W' = 6 \text{ mL}\cdot\text{h}^{-1}$). In Fig. 7, the variation of the predicted diffusion coefficients D_B is reported as a function of the axial position z . It can be observed that, for both conditions, the value of D_B decreases as z increases, and then converges towards a plateau for z greater than 4 mm. This indicates that the fitting between the experimental and theoretical concentration profiles must be done relatively far from the outlet of the capillary, namely only for axial positions z for which the edge of the colored flow starts to be parallel to the wall of the tube. Note that, this plateau is reached at smaller axial positions for ($Q_R' = 3 \text{ mL}\cdot\text{h}^{-1}$, $Q_W' = 6 \text{ mL}\cdot\text{h}^{-1}$) than for $Q_R' = 9 \text{ mL}\cdot\text{h}^{-1}$ / $Q_W' = 9 \text{ mL}\cdot\text{h}^{-1}$; this could be explained by the conic structure of the flow which is more stable/horizontal in the latter operating condition. For both conditions, after the $z = 4 \text{ mm}$ position, the optimization procedure gives a value of the diffusion coefficient of dihydroresorufin $D_B = (8.65 \pm 0.21) \times 10^{-11} \text{ m}^2\cdot\text{s}^{-1}$. This value is in agreement with the orders of magnitude of the diffusion coefficients of dye classically reported in the literature: for example, the diffusion coefficient of “meta” benzopurpurine in 0.002 M NaOH solution⁴¹ is $3.15 \times 10^{-10} \text{ m}^2\cdot\text{s}^{-1}$, and the one of methylene blue in 0.01 M NaCl solution⁴² being $1.2 \times 10^{-10} \text{ m}^2\cdot\text{s}^{-1}$.

Diffusion coefficient of oxygen D_{O_2} in the dye solution

Fig. 8 (a) shows a typical image illustrating the diffusion of O_2 in the dye solution ($Q_R'' = 9 \text{ mL}\cdot\text{h}^{-1}$, $Q_W'' = 9 \text{ mL}\cdot\text{h}^{-1}$): the pink color represents the areas where the two solutions (deionized water saturated with O_2 and dihydroresorufin solution) enter into contact and react. As observed previously, for the measurement of D_B , the edge of the colored flow is not parallel to the wall of the tube at the initial stage (i.e. close the outlet of the capillary), due to the occurrence of some convective effects; afterwards, the

profile becomes parallel, indicating a pure diffusion of oxygen from the inner flow to the surrounding. As a consequence, here also, in order to determine an appropriate value of D_{O_2} , adequate axial positions should be chosen as initial moment for simulation ($t = 0$ s). An axial position of $z = 2.30$ mm has been selected.

As shown in Fig. 8 (b), the radial profile of grey values presents a more complicated shape for the diffusion of oxygen in the dye solution than for the one of dihydroresorufin in deionized water. Indeed, it consists of three parts: two peaks and one central plateau between the two peaks. The peaks correspond to the highest gradients of the concentration of O_2 , and thus represent the main contribution to the overall diffusion process. The predicted value of D_{O_2} corresponding to the profiles reported in Fig. 8 (b) equals to $5 \times 10^{-7} \text{ m}^2 \text{ s}^{-1}$; it is two orders of magnitude larger than the one in literature³², this indicating that, at this axial location ($z = 2.30$ mm), the mechanism is not purely diffusive.

Fig. 9 compares the experimental radial profiles of grey values (proportional to equivalent concentrations of O_2) at an axial position z of 4.59 mm with the simulated ones for different values of diffusion coefficients D_{O_2} . It can be observed that the impact of these latter is not the same, depending on that whether the peak areas or the plateau area is considered. Given that the peaks represent the main contribution to the diffusion process, a compromise amongst the fitting qualities of the three parts has to be found. For that, the peak thickness, noted as $\delta_{0.9}$, corresponding to a normalized grey value $GV^* = 0.9$, has been chosen for a comparison purpose. Their experimental and predicted values are reported in Table 2a at an axial position z of 4.59 mm. It can be seen that the deviation between the experimental $\delta_{0.9}$ and the simulated one is minimal when $D_{O_2} = 3.2 \times 10^{-9} \text{ m}^2 \cdot \text{s}^{-1}$.

To further verify the reliability of this value of D_{O_2} , two other axial locations, $z = 3.06$ mm and $z = 3.82$ mm, were tested for the operation condition corresponding to $Q_R = 9 \text{ mL} \cdot \text{h}^{-1}$, $Q_W = 9 \text{ mL} \cdot \text{h}^{-1}$. As depicted in Fig. 10, the best fitting quality between experimental and predicted profiles is obtained for the

highest axial location ($z = 4.59$ mm). This confirms that the procedure should be applied relatively far from the outlet of the capillary, to avoid any distortion due to convective effects.

For this optimal axial location z of 4.59 mm, the same fitting procedure has been applied for two other operating conditions, ($Q_R'' = 4.5 \text{ mL}\cdot\text{h}^{-1}$, $Q_W'' = 9 \text{ mL}\cdot\text{h}^{-1}$) and ($Q_R'' = 3 \text{ mL}\cdot\text{h}^{-1}$, $Q_W'' = 6 \text{ mL}\cdot\text{h}^{-1}$); the results are presented in terms of peak thickness $\delta_{0,9}$ in Table 2b and 2c. For both conditions, the best fitting is obtained for D_{O_2} equals to $3.2 \times 10^{-9} \text{ m}^2\cdot\text{s}^{-1}$. The variations of the predicted diffusion coefficients D_{O_2} as a function of the axial location z are plotted in Fig. 11 for different operating conditions. As previously observed for the diffusion coefficient of dihydroresorufin D_B , for both conditions, D_{O_2} decreases strongly as z increases, and converges towards a plateau for z larger than 4 mm. At last, by optimizing both the conditions, one finds $D_{O_2} = (3.2 \pm 0.1) \times 10^{-9} \text{ m}^2\cdot\text{s}^{-1}$. This value D_{O_2} has the same order of magnitude D_{O_2} than the one in pure water, $1.75 \times 10^{-9} \text{ m}^2\cdot\text{s}^{-1}$, reported in the literature^{32,44}. A more advanced comparison with literature data remains difficult as the present liquid phase composition is specific (sodium hydroxide, glucose and resazurin). One can yet mention the value of $3.5 \times 10^{-9} \text{ m}^2\cdot\text{s}^{-1}$, reported by Yano et al⁴⁵ for the diffusion of oxygen in 0.1 M KOH solution.

Hatta number Ha and enhancement factor E

Thanks to the knowledge of the diffusion coefficients of O_2 ($D_{O_2} = (3.2 \pm 0.1) \times 10^{-9} \text{ m}^2\cdot\text{s}^{-1}$) and of dihydroresorufin ($D_B = (8.65 \pm 0.21) \times 10^{-11} \text{ m}^2\cdot\text{s}^{-1}$), the enhancement factor associated with the colorimetric reaction can be calculated using Eq. (13). Considering a concentration of dihydroresorufin in the liquid bulk C_{Bb} equals to $5.1 \times 10^{-4} \text{ mol}\cdot\text{L}^{-1}$ and a concentration of oxygen at saturation $C_{O_2}^*$ to $2.55 \times 10^{-4} \text{ mol}\cdot\text{L}^{-1}$, it leads to:

$$E_i = 1 + \frac{C_{Bb} \cdot D_B}{\nu \cdot C_{O_2}^* \cdot D_{O_2}} = 1.03 \pm 0.01 \quad (24)$$

To verify that the approximated solution proposed by Van Krevelen and Hoftijzer (Eq. 14) for fast reaction in the diffusional film can be applied in the present conditions, the Hatta number should be calculated. The use of Eq. (14) requires the knowledge of the reaction kinetics constant, k_2 and the liquid-side mass transfer coefficient, k_L . The constant k_2 can be deduced from the reaction characteristic time t_{react} . As only its maximum value has been determined ($t_{react} \leq 7.2$ ms, see section “Reaction characteristic time”), only the minimum value of the reaction constant k_2 can be calculated as follows:

$$(k_2)_{\min} = \frac{1}{\nu \cdot (t_{react})_{\max} \cdot C_{O_2}^*} = 2.72 \times 10^5 \text{ L} \cdot (\text{mol} \cdot \text{s})^{-1} \quad (25)$$

The liquid side mass transfer coefficient k_L depends on the system scale under study. For micro/milli reactors, an order of magnitude of $10^{-4} \text{ m} \cdot \text{s}^{-1}$ can be reasonably considered^{7,8}. At last, one finds a minimal value of the Hatta number equals to:

$$(Ha)_{\min} = \frac{\sqrt{(k_2)_{\min} \cdot C_{Bb} \cdot D_{O_2}}}{k_L} = 6.66 \quad (26)$$

The value being higher than 3, $Ha > 3$, the approximated solution proposed by Van Krevelen and Hoftijzer¹⁹ (see Eq. 14) can be rigorously applied. It leads to a value of the enhancement factor close to the unity, $E = 1.03$. This demonstrates that even if the colorimetric reaction is fast, and even quasi-instantaneous, there is no enhancement of the gas-liquid mass transfer by the reaction in the conditions (C_{Bb} , milli/microreactors) for which it has been implemented. Such a result is opposite to the general knowledge that high Ha lead to high E ; it is the consequence of the fact that the diffusion of the dye

(dihydroresorufin) in the liquid film is too slow ($D_B = 8.65 \times 10^{-11} \text{ m}^2 \cdot \text{s}^{-1}$) compared to the diffusion of oxygen ($D_{O_2} = 3.2 \times 10^{-9} \text{ m}^2 \cdot \text{s}^{-1}$), and thus prevents the reaction to occur in the liquid film.

At last, it is interesting to define some guidelines enabling to evaluate the conditions required to implement the colorimetric method at other scales or in other gas-liquid systems. For that, one should guarantee that no enhancement of the gas-liquid mass transfer occurs. This implies that the initial concentration of resazurin C_{Bb} to be used should be carefully chosen. To meet this requirement, the minimum recommended $(C_{Bb})_{rec,min}$ and the associated E , which correspond to $Ha = 3$, are plotted in Fig. 12 as a function of the expected magnitude of the liquid side mass transfer coefficient k_L in the milli/micro systems under test. It can be observed that $(C_{Bb})_{rec,min}$ is exponentially proportional to the order of the magnitude of k_L . In particular, in microstructured systems, where k_L can be higher than $10^{-3} \text{ m} \cdot \text{s}^{-1}$, $(C_{Bb})_{rec,min}$ could become very high and makes the colorimetric technique no more applicable for solubility reasons; simultaneously, the enhancement factor E becomes higher than 1 (until 1.8), which means that the experimental result should be corrected by E to obtain the intrinsic k_L . These findings shows that, to keep E smaller than 1.1, which is a tolerable value with respect to the accuracy of the technique (around 13%)¹, the magnitude of k_L for implementing this colorimetric technique should be approximately below $4.5 \times 10^{-4} \text{ m} \cdot \text{s}^{-1}$.

However, these trends should be taken with caution as only a maximum reaction characteristic time of the oxygen colorimetric reaction was acquired (7.2 ms). It can be known from Eq. (25) and (26) that k_2 is inversely proportional to reaction characteristic time t_{react} , and Ha is proportional to k_2 and C_{Bb} . Therefore, if t_{react} is in reality smaller than 7.2 ms, $(C_{Bb})_{rec,min}$ can be correspondingly decreased. Fig. 12 also plots the tendencies of $(C_{Bb})_{rec,min}$ and E under assumed smaller t_{react} , 1 ms, 3 ms and 5 ms. The

strong impact of t_{react} on $(C_{Bb})_{rec,min}$ and on E is clearly observed: the values of these two parameters are significantly decreased. In particular, if the real t_{react} equals to 1 ms, $(C_{Bb})_{rec,min}$ stays low, and E is almost independent of the studied k_L and close to one: in these conditions, the colorimetric technique could be applied without any restriction in most milli/micro systems involving larger range of k_L .

Conclusion

This paper presented original optical methods to determine the Hatta number Ha and the enhancement factor E associated with the colorimetric reaction proposed by Dietrich et al. (2013)¹ to visualize and locally characterize the gas-liquid mass transfer. It was based on the combination of specific experiments in microstructured devices with modelling approaches. They enabled the maximal characteristic time of the fast reaction to be determined and as well as the diffusion coefficients of the dye (dihydroresorufin) and O_2 . It was demonstrated that the oxygen colorimetric reaction was instantaneous and no enhancement of the gas-liquid mass transfer by this extremely fast reaction occurred as E was found equal to 1.03 ± 0.01 . This result, opposite to the general knowledge, can be explained by the fact that the relative large molecular structure of dihydroresorufin limits its diffusion into the film, and thus prevent the reaction to occur in the liquid film. Some guidelines enabling to evaluate the conditions required to implement the colorimetric method at other scales or in other gas-liquid systems were also given. In the future, specific effort should be paid to determine more precisely the real characteristic time of this fast reaction, as this parameter has a strong effect on the enhancement factor.

Acknowledgments

The financial assistance provided by the China Scholarship Council for L. Yang is gratefully acknowledged.

Notations

C	=	concentration, $\text{mol} \cdot \text{m}^{-3}$
D	=	diffusion coefficient, $\text{m}^2 \cdot \text{s}^{-1}$
d	=	diameter, m
GV	=	grey value
GV^*	=	normalized grey value
k_2	=	reaction constant, $\text{m}^3 \cdot (\text{mol} \cdot \text{s})^{-1}$
k_L	=	liquid side mass transfer coefficient, $\text{m} \cdot \text{s}^{-1}$
Q	=	volumetric flow rate, $\text{m}^3 \cdot \text{s}^{-1}$
r	=	radial position, m
r_B, r_{O_2}	=	consumption rate of dihydroresorufin and oxygen, $\text{mol} \cdot \text{m}^3 \cdot \text{s}^{-1}$
t_{react}	=	reaction characteristic time, s
u	=	liquid velocity in the micromixer, $\text{m} \cdot \text{s}^{-1}$
z	=	axial position, m

Greek letters

ν	=	stoichiometry coefficient
μ_L	=	dynamic viscosity of the dye solution, $\text{Pa} \cdot \text{s}$
μ_L'	=	dynamic viscosity of the deionized water, $\text{Pa} \cdot \text{s}$
ρ_L	=	density of the dye solution, $\text{kg} \cdot \text{m}^{-3}$
ρ_L'	=	density of the deionized water, $\text{kg} \cdot \text{m}^{-3}$
σ_L	=	surface tension of the dye solution, $\text{N} \cdot \text{m}^{-1}$
σ_L'	=	surface tension of the deionized water, $\text{N} \cdot \text{m}^{-1}$
φ	=	transferred mass flux of oxygen, $\text{kg} \cdot \text{m}^{-3} \cdot \text{s}^{-1}$

Dimensionless numbers

E	=	enhancement factor
Ca	=	Capillary number, $=\mu_L \cdot u / \sigma_L$
Ha	=	Hatta number, $Ha^2 = D_{O_2} \cdot k_2 \cdot C_{Bb} / k_L^2$
Re	=	Reynold number, $=\rho_L \cdot d_h \cdot u / \mu_L$
Da	=	Damköhler number, $=k_L \cdot a \cdot \tau$

Subscripts

0	=	background
---	---	------------

B	=	concentration (or diffusion coefficient) of dihydroresorufin
Bb	=	dihydroresorufin in the bulk
c	=	capillary
i	=	enhancement factor for instantaneous reaction
in	=	inner diameter
m	=	mixing time
max	=	maximum value
out	=	outer diameter
R	=	dye solution
r	=	residence time
t	=	PTFE tube
w	=	deionized water

Literature Cited

1. Dietrich N, Loubière K, Jimenez M, Hébrard G, Gourdon C. A new direct technique for visualizing and measuring gas–liquid mass transfer around bubbles moving in a straight millimetric square channel. *Chem Eng Sci.* 2013;100:172-182.
2. Kherbeche A, Milnes J, Jimenez M, Dietrich N, Hébrard G, Lekhlif B. Multi-scale analysis of the influence of physicochemical parameters on the hydrodynamic and gas–liquid mass transfer in gas/liquid/solid reactors. *Chem Eng Sci.* 2013;100:515-528.
3. Yang L, Dietrich N, Loubière K, Gourdon C, Hébrard G. Visualization and characterization of gas–liquid mass transfer around a Taylor bubble right after the formation stage in microreactors. *Chem Eng Sci.* 2016;143:364-368.
4. Leclerc A, Alamé M, Schweich D, Pouteau P, Delattre C, de Bellefon C. Gas–liquid selective oxidations with oxygen under explosive conditions in a micro-structured reactor. *Lab Chip.* 2008;8(5):814-817.
5. Vanoye L, Wang J, Pablos M, Philippe R, Bellefon C de, Favre-Réguillon A. Continuous, Fast, and Safe Aerobic Oxidation of 2-Ethylhexanal: Pushing the Limits of the Simple Tube Reactor

for a Gas/Liquid Reaction. *Org Process Res Dev.* 2016;20(1):90-94.

6. Darvas F, Dorman G, Hessel V. *Flow Chemistry*. Berlin: Boston : De Gruyter Textbook; 2014.
7. Su Y, Hessel V, Noël T. A compact photomicroreactor design for kinetic studies of gas-liquid photocatalytic transformations. *AIChE J.* 2015;61(7):2215-2227.
8. Shvydkiv O, Limburg C, Nolan K, Oelgemöller M. Synthesis of Juglone (5-Hydroxy-1,4-Naphthoquinone) in a Falling Film Microreactor. *J Flow Chem.* 2012;2(2):52-55.
9. Roudet M, Loubiere K, Gourdon C, Cabassud M. Hydrodynamic and mass transfer in inertial gas-liquid flow regimes through straight and meandering millimetric square channels. *Chem Eng Sci.* 2011;66(13):2974-2990.
10. Sobieszuk P, Aubin J, Pohorecki R. Hydrodynamics and Mass Transfer in Gas-Liquid Flows in Microreactors. *Chem Eng Technol.* 2012;35(8):1346-1358.
11. Ganapathy H, Al-Hajri E, Ohadi M. Mass transfer characteristics of gas-liquid absorption during Taylor flow in mini/microchannel reactors. *Chem Eng Sci.* 2013;101:69-80.
12. Yang L, Tan J, Wang K, Luo G. Mass transfer characteristics of bubbly flow in microchannels. *Chem Eng Sci.* 2014;109:306-314.
13. Mikaelian D, Haut B, Scheid B. Bubbly flow and gas-liquid mass transfer in square and circular microchannels for stress-free and rigid interfaces: dissolution model. *Microfluid Nanofluidics.* 2015;19(4):899-911.
14. Tan J, Lu YC, Xu JH, Luo GS. Mass transfer characteristic in the formation stage of gas-liquid segmented flow in microchannel. *Chem Eng J.* 2012;185-186:314-320.
15. Erb RE, Ehlers MH. Resazurin Reducing Time as an Indicator of Bovine Semen Fertilizing Capacity. *J Dairy Sci.* 1950;33(12):853-864.

16. O'Brien J, Wilson I, Orton T, Pognan F. Investigation of the Alamar Blue (resazurin) fluorescent dye for the assessment of mammalian cell cytotoxicity. *Eur J Biochem.* 2000;267(17):5421-5426.
17. Anderson L, Wittkopp SM, Painter CJ, et al. What Is Happening When the Blue Bottle Bleaches: An Investigation of the Methylene Blue-Catalyzed Air Oxidation of Glucose. *J Chem Educ.* 2012;89(11):1425-1431.
18. Zhang Y, Song P, Fu Q, Ruan M, Xu W. Single-molecule chemical reaction reveals molecular reaction kinetics and dynamics. *Nat Commun.* 2014; vol. 5:4238.
19. van Krevelen DW, Hoftijzer PJ. Kinetics of gas-liquid reactions part I. General theory. *Recl des Trav Chim des Pays-Bas.* 1948;67(7):563-586.
20. Hikita H, Asai S, Ishikawa H, Honda M. The kinetics of reactions of carbon dioxide with monoethanolamine, diethanolamine and triethanolamine by a rapid mixing method. *Chem Eng J.* 1977;13(1):7-12.
21. Astaria G, Savage DW, Bisio A. *Gas Treating with Chemical Solvents.* J. Wiley and Sons, New York; 1983.
22. Yoshida J. *Basics of Flow Microreactor Synthesis.* Tokyo: Springer Japan; 2015.
23. Hecht K, Kraut M, Kölbl A. Microstructured mixing devices: an efficient tool for the determination of chemical kinetic data? *AIChE Spring Meet Houston, Texas, USA.* 2007;(4):22-26.
24. Wang P, Wang K, Zhang J, Luo G. Kinetic study of reactions of aniline and benzoyl chloride in a microstructured chemical system. *AIChE J.* 2015;61(11):3804-3811.
25. Hauf W, Grigull U. Optical methods in heat transfer. In: Hartnett JP, Thomas F, Irvine J, eds. *Advances in Heat Transfer, Vol. 6.* Vol New York: Academic Press; 1970.
26. Ambrosini D, Paoletti D, Rashidnia N. Overview of diffusion measurements by optical

- techniques. *Opt Lasers Eng.* 2008;46(12):852-864.
27. Taylor G. Dispersion of Soluble Matter in Solvent Flowing Slowly through a Tube. *Proc R Soc A Math Phys Eng Sci.* 1953;219(1137):186-203.
 28. Ruiz-Bevia F, Fernandez-Sempere J, Celdran-Mallol A, Santos-Garcia C. Liquid diffusion measurement by holographic interferometry. *Can J Chem Eng.* 1985;63(5):765-771.
 29. Mohan N, Rastogi P. Recent developments in digital speckle pattern interferometry. *Opt Lasers Eng.* 2003;40:439-588.
 30. Jimenez M, Dietrich N, Cockx A, Hébrard and G. Experimental study of O₂ diffusion coefficient measurement at a planar gas-liquid interface by planar laser-induced fluorescence with inhibition. *AIChE J.* 2013;59(1):325-333.
 31. Winkler LW. Die Bestimmung des im Wasser gelösten Sauerstoffes. *Berichte der Dtsch Chem Gesellschaft.* 1888;21(2):2843-2854.
 32. Galambos P, Forster FK. Micro-Fluidic Diffusion Coefficient Measurement. In: *Micro Total Analysis Systems '98.* Vol Dordrecht: Springer Netherlands; 1998:189-192.
 33. Kamholz AE, Schilling EA, Yager P. Optical Measurement of Transverse Molecular Diffusion in a Microchannel. *Biophys J.* 2001;80(4):1967-1972.
 34. Fick A. Ueber Diffusion. *Ann der Phys und Chemie.* 1855;170(1):59-86.
 35. Crank J. *The Mathematics of Diffusion.* 2nd ed. England: Clarendon Press, Oxford; 1975.
 36. Jimenez M, Dietrich N, Grace JR, Hébrard G. Oxygen mass transfer and hydrodynamic behaviour in wastewater: Determination of local impact of surfactants by visualization techniques. *Water Res.* 2014;58:111-121.
 37. Culbertson C. Diffusion coefficient measurements in microfluidic devices. *Talanta.*

2002;56(2):365-373.

38. Quinn J a., Lin CH, Anderson JL. Measuring diffusion coefficients by Taylor's method of hydrodynamic stability. *AIChE J.* 1986;32(12):2028-2033.
39. Kuzmin D. *A Guide to Numerical Methods for Transport Equations.* Erlangen; 2010.
40. Falk L, Commenge J-M. Performance comparison of micromixers. *Chem Eng Sci.* 2010;65(1):405-411.
41. Robinson C. The Diffusion Coefficients of Dye Solutions and their Interpretation. *Proc R Soc Lond A Math Phys Sci.* 1935;148(865):681-695.
42. Leaist DG. The effects of aggregation, counterion binding, and added sodium chloride on diffusion of aqueous methylene blue. *Can J Chem.* 1988;66(9):2452-2457.
43. Wilke CR, Chang P. Correlation of diffusion coefficients in dilute solutions. *AIChE J.* 1955;1(2):264-270.
44. Yano T. Electrochemical Behavior of Highly Conductive Boron-Doped Diamond Electrodes for Oxygen Reduction in Alkaline Solution. *J Electrochem Soc.* 1998;145(6):1870.

Table 1 Physiochemical properties of the liquid phases at 293.15K.

Liquid phase	C (kg·m ⁻³)	σ_L (mN·m ⁻¹)	μ_L (mPa·s)	ρ_L (kg·m ⁻³)	C^* (mg·L ⁻¹)
Deionized water	0	71.4	1.003	996.8	9.05
Aqueous solution of glucose anhydrous and sodium hydroxide	20 20	76	1.118	1004.5	8.15 ¹
Aqueous solution of glucose anhydrous sodium hydroxide and resazurin	20 20 0.1	75	1.118	1004.5	-

Table 2 Diffusion peak thickness at normalized concentration of O₂ equal to 0.9, $\delta_{0.9}$: comparison between simulation and experimental values (axial distance $z = 4.59$ mm). Experimental operating conditions: a. $Q_R'' = 9 \text{ mL}\cdot\text{h}^{-1}$, $Q_W'' = 9 \text{ mL}\cdot\text{h}^{-1}$; b. $Q_R'' = 4.5 \text{ mL}\cdot\text{h}^{-1}$, $Q_W'' = 9 \text{ mL}\cdot\text{h}^{-1}$; c. $Q_R'' = 3 \text{ mL}\cdot\text{h}^{-1}$, $Q_W'' = 6 \text{ mL}\cdot\text{h}^{-1}$.

a				
$D_{O_2} (\text{m}^2 \cdot \text{s}^{-1})$	3.2×10^{-10}	3.2×10^{-9}	3.2×10^{-8}	$\delta_{0.9,exp} (\text{mm})$
$\delta_{0.9} (\text{mm})$	0.020	0.032	0.058	0.030
Deviation	33.33%	6.67%	93.33%	
b				
$D_{O_2} (\text{m}^2 \cdot \text{s}^{-1})$	3.2×10^{-10}	3.2×10^{-9}	3.2×10^{-8}	$\delta_{0.9,exp} (\text{mm})$
$\delta_{0.9} (\text{mm})$	0.024	0.028	0.057	0.029
Deviation	17.24%	3.45%	96.55%	
c				
$D_{O_2} (\text{m}^2 \cdot \text{s}^{-1})$	3.2×10^{-10}	3.2×10^{-9}	3.2×10^{-8}	$\delta_{0.9,exp} (\text{mm})$
$\delta_{0.9} (\text{mm})$	0.022	0.030	0.059	0.031
Deviation	29.03%	3.23%	90.32%	

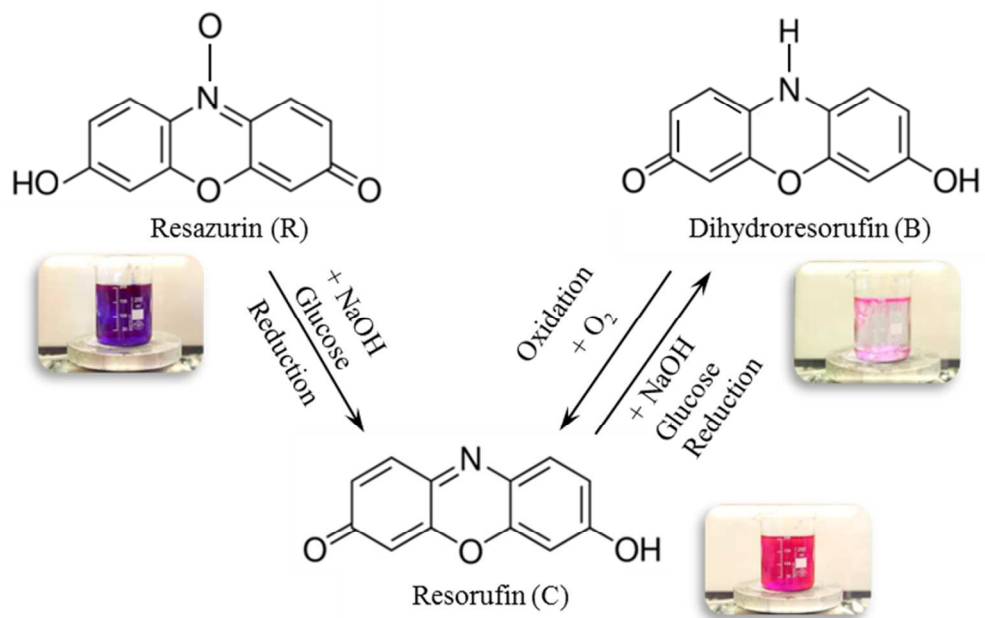


Fig. 1 Reaction scheme for the reversible oxidation-reduction colorimetric reactions between resorufin and dihydroresorufin. The oxidation reaction is quasi-instantaneous, and the reduction reaction is slow (few minutes).

82x52mm (300 x 300 DPI)

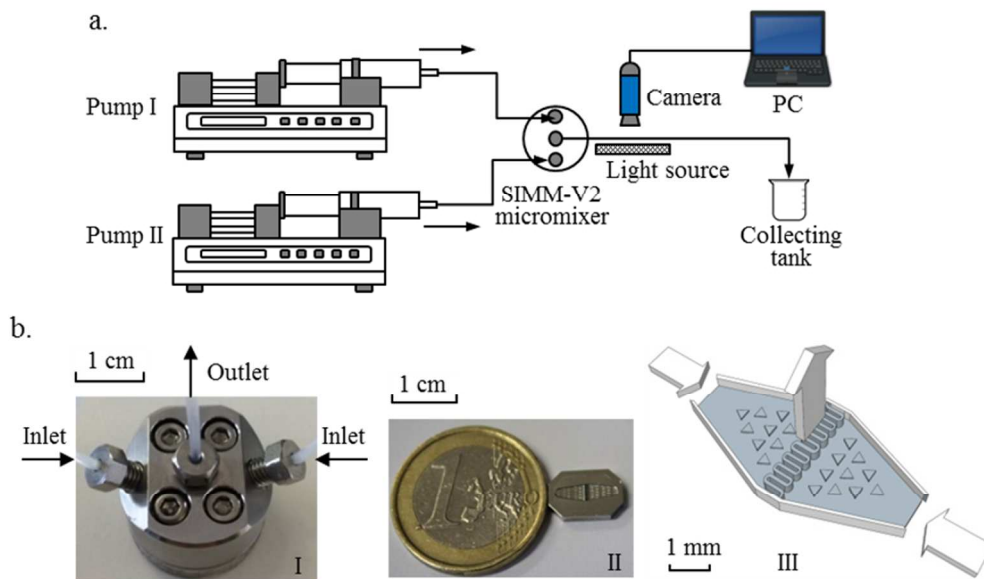


Fig. 2 (a) Schematic diagram of micromixer experiment. Pump I: neMESYS high pressure syringe pump for deionized water saturated with O₂; pump II: neMESYS high pressure syringe pump for dye solution (nitrogen flushed). (b) Picture (I); inner structure (II); illustration of the mixing channel (45×200μm) (III) of SIMM-V2 micromixer.

82x49mm (300 x 300 DPI)

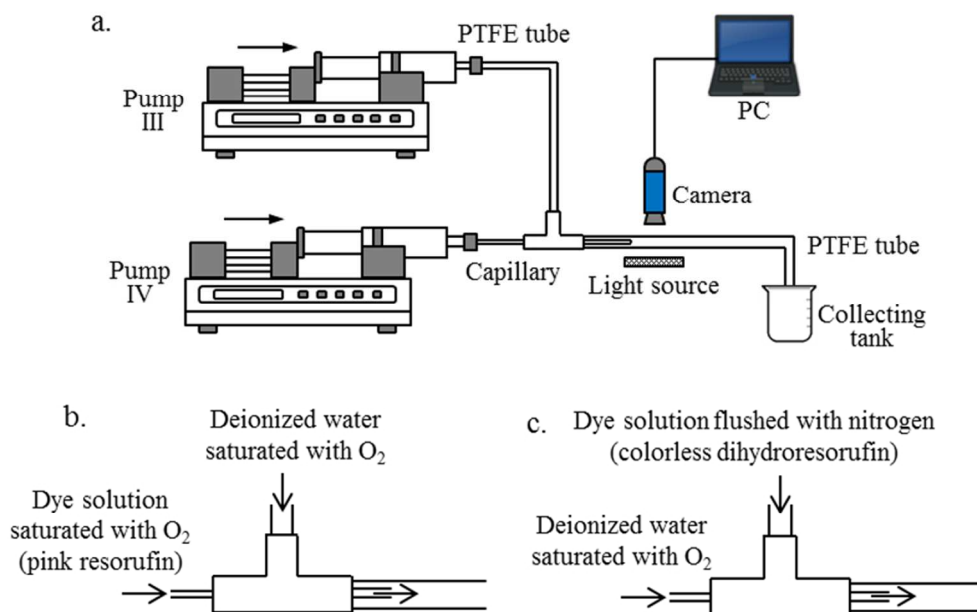


Fig. 3 (a) Experimental set-up for the measurement of diffusion coefficients: general overview. Schematic diagram at the connector for measuring (b) and (c).

82x51mm (300 x 300 DPI)

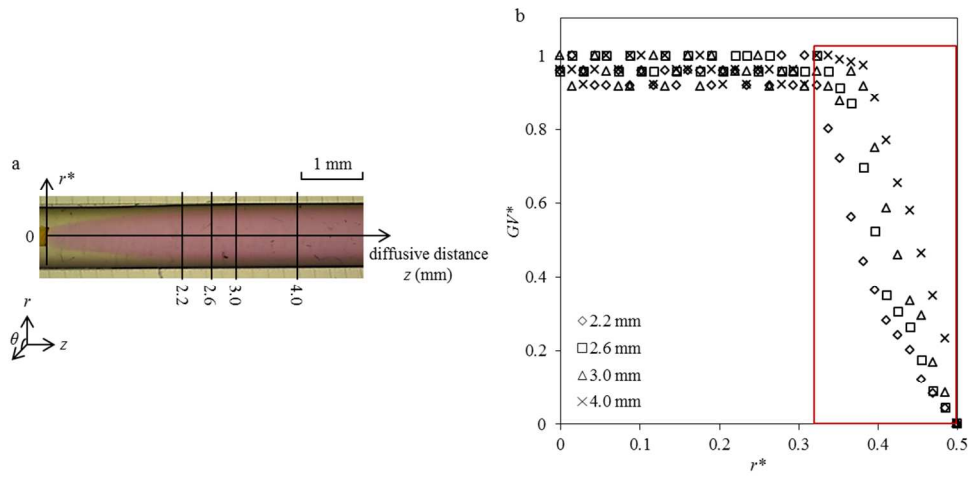


Fig. 4 Experiments related to the measurement of the diffusion coefficient of dihydroresorufin . (a) Typical image representing the evolution of color intensity distribution inside the tube. (b) Normalized radial profile of grey values (proportional to the normalized concentration of resorufin) for various axial positions z . ($U = 3 \text{ mL}\cdot\text{h}^{-1}$, $U_0 = 6 \text{ mL}\cdot\text{h}^{-1}$; $Re' = 3.82$). The experimental data in the red rectangular are the ones that will be used afterwards for the comparison with the theoretical profiles.

103x49mm (300 x 300 DPI)

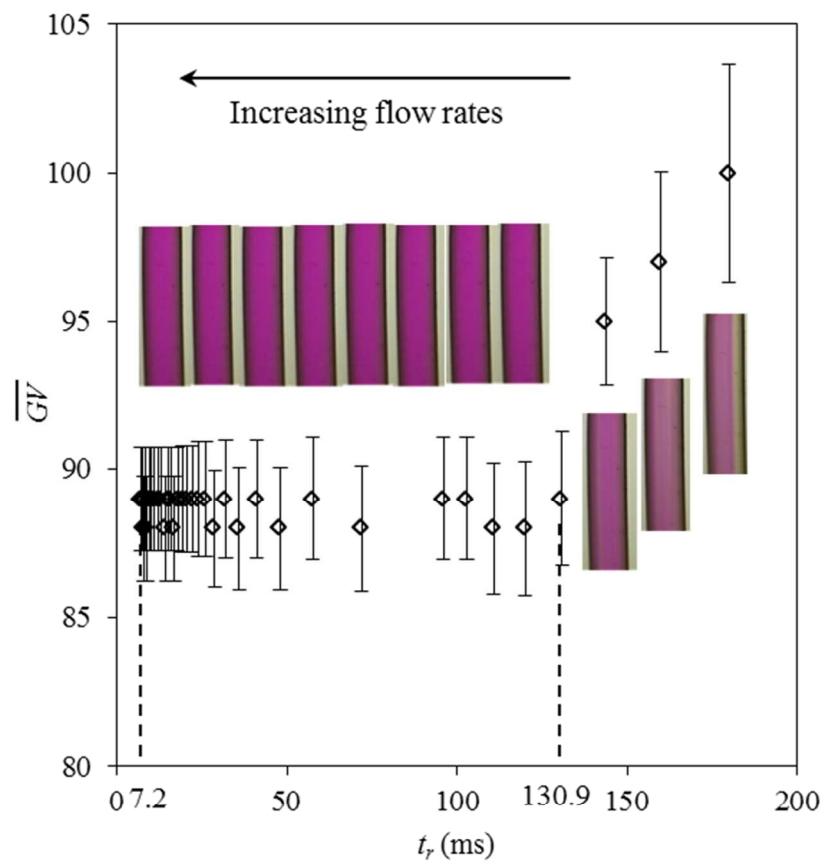


Fig. 5 Variation of the average grey value at the outlet of the micromixer as a function of the residence time in the micromixer t_r . The bars represent the experimental deviations associated to

82x74mm (300 x 300 DPI)

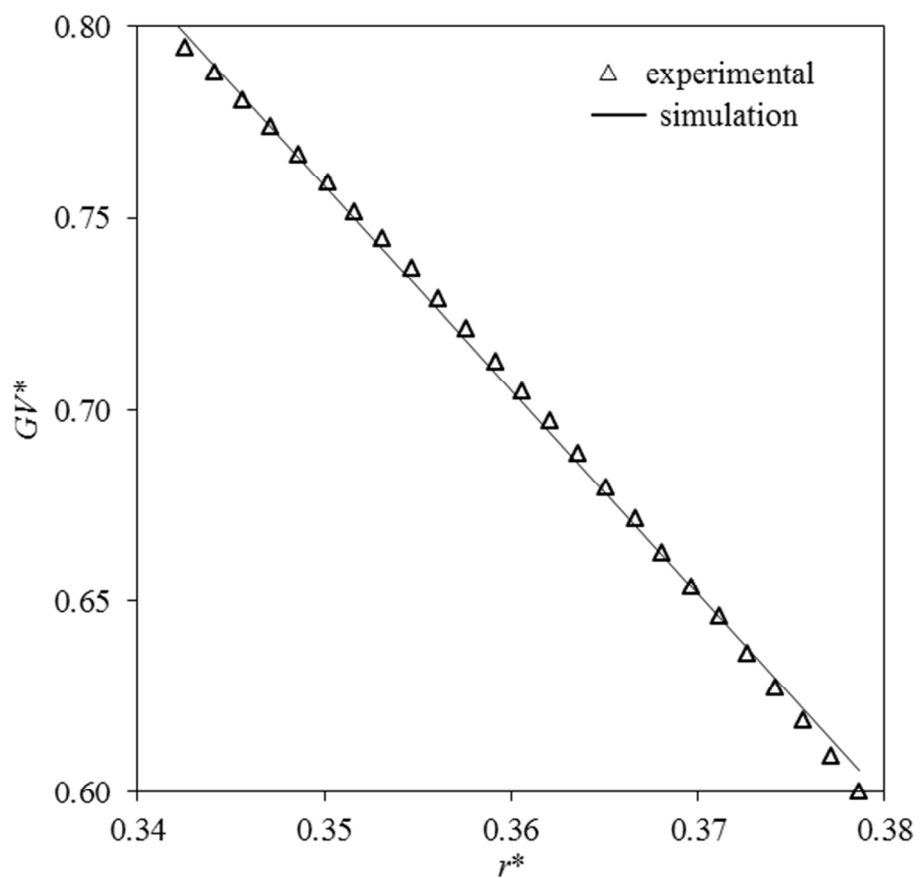


Fig. 6 Determination of the diffusion coefficient of dihydroresorufin: comparison of the experimental radial profiles of normalized grey values with the predicted ones at an axial location $z = 2.6$ m, and for $Q = 3$ mL·h⁻¹, $v = 6$ mL·h⁻¹. The associated predicted diffusion coefficient is equal to $D = 2.25 \times 10^{-9}$ m²·s⁻¹.

82x75mm (300 x 300 DPI)

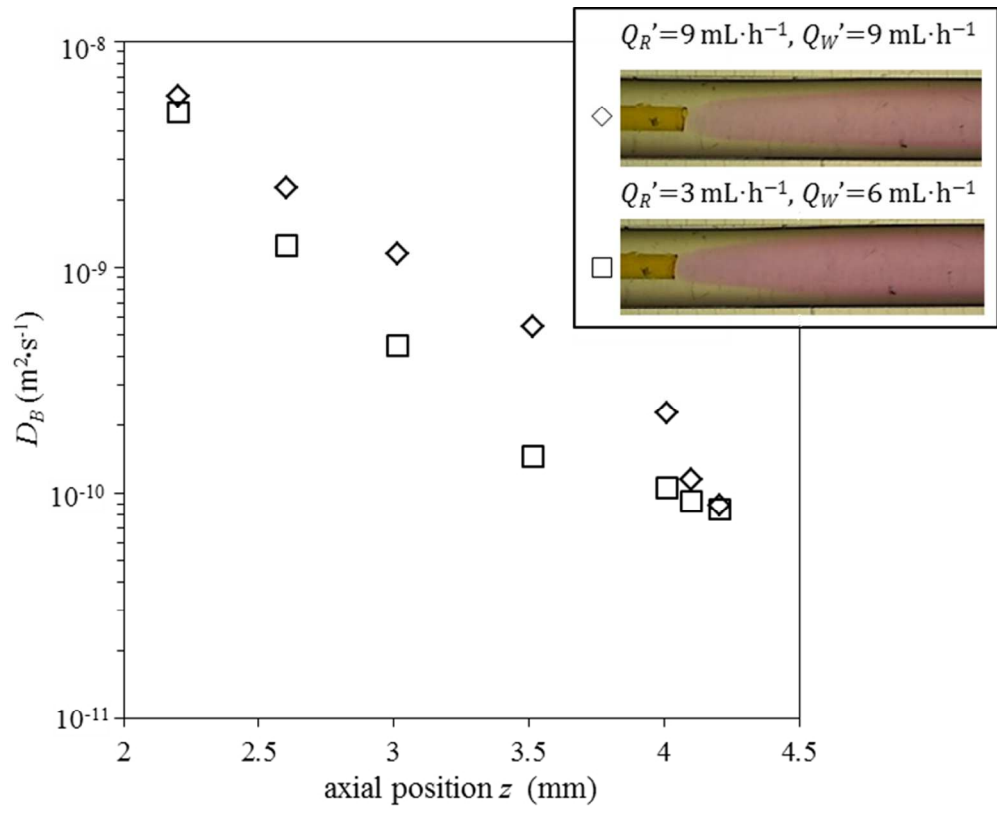


Fig. 7 Determination of the diffusion coefficient of dihydroresorufin: variation of the predicted as a function of the axial position z .

82x66mm (300 x 300 DPI)

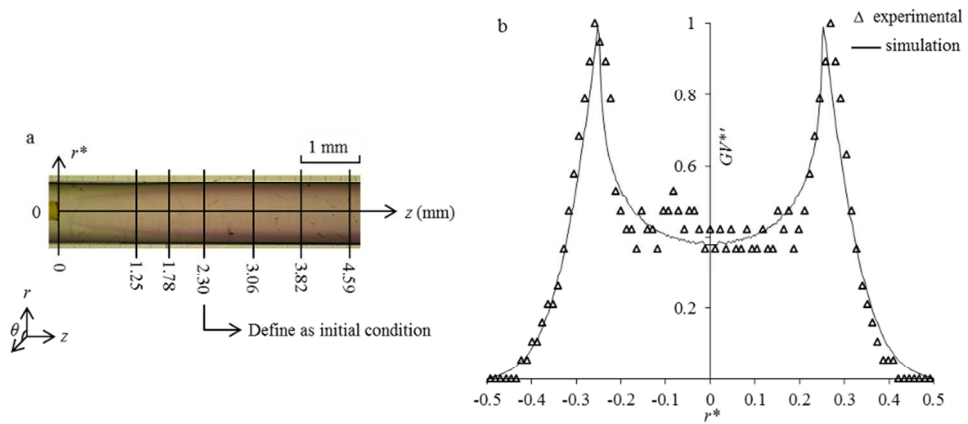


Fig. 8 Determination of the diffusion coefficient of oxygen: (a) Typical experimental image representing the diffusion of O₂ in the dye solution; (b) Comparison between the experimental radial profile of the normalized grey values with the predicted one at an axial location $z = 2.30$ mm and for $Q = 9$ mL·h⁻¹, $v = 9$ mL·h⁻¹. The associated predicted value of diffusion coefficient is $D = 5 \times 10^{-7}$ m²·s⁻¹.

82x38mm (300 x 300 DPI)

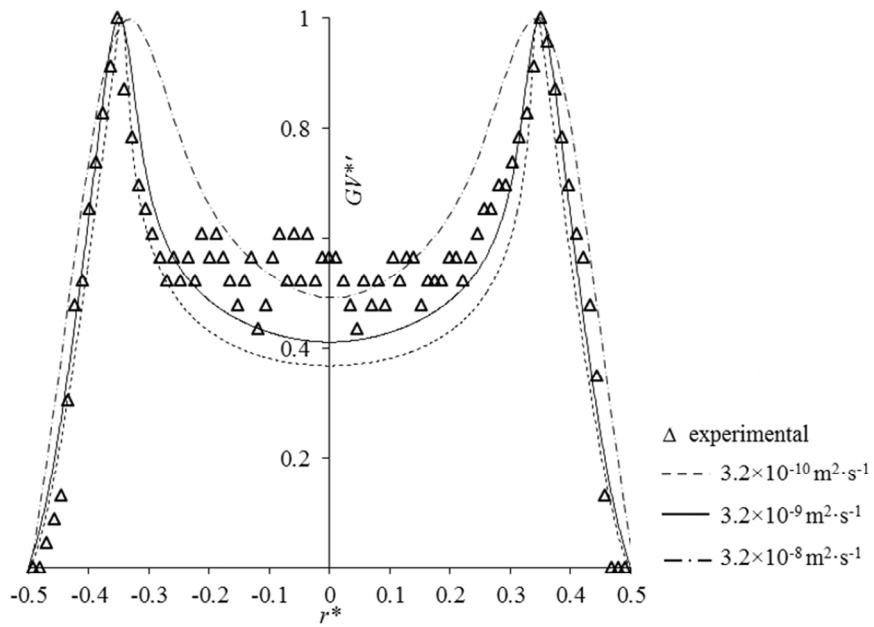


Fig. 9 Determination of the diffusion coefficient of oxygen: comparison between the experimental radial profiles of the normalized grey values with the predicted ones at an axial location $z = 4.59 \text{ mm}$ for different values of $(= 9 \text{ mL} \cdot \text{h}^{-1}, = 9 \text{ mL} \cdot \text{h}^{-1})$.

82x57mm (300 x 300 DPI)

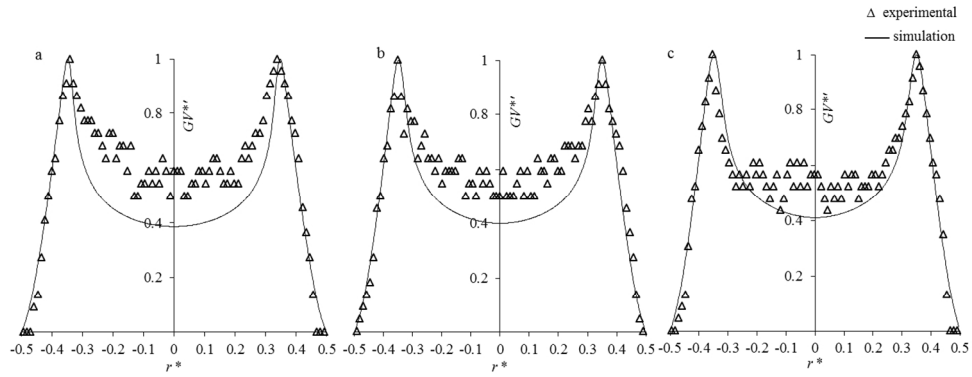


Fig. 10 Determination of the diffusion coefficient of oxygen: comparison between the experimental radial profiles of the normalized grey values with the predicted ones for a predicted value of equal to $3.2 \times 10^{-9} \text{ m}^2 \cdot \text{s}^{-1}$ and for different axial positions z . (a) $z = 3.06 \text{ mm}$. (b) $z = 3.82 \text{ mm}$. (c) $z = 4.59 \text{ mm}$. ($\dot{V} = 9 \text{ mL} \cdot \text{h}^{-1}$, $\dot{V}_1 = 9 \text{ mL} \cdot \text{h}^{-1}$).

122x48mm (300 x 300 DPI)

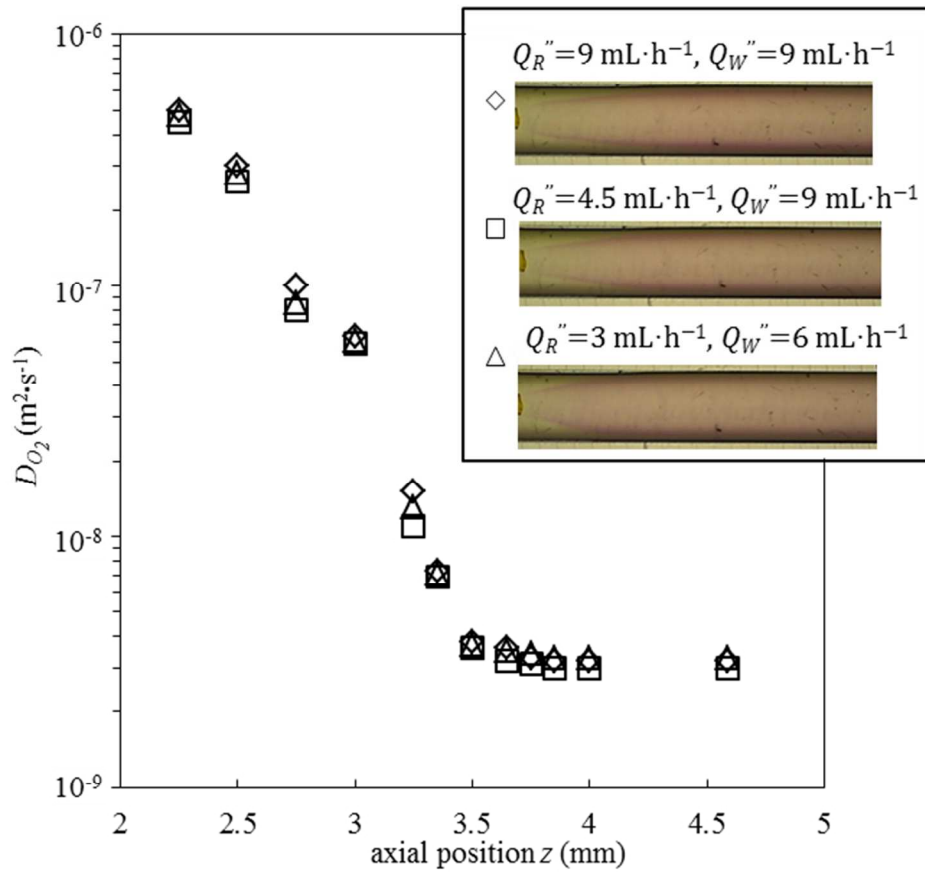


Fig. 11 Variation of the diffusion coefficient of oxygen as a function of axial position z for different operating conditions.

82x74mm (300 x 300 DPI)

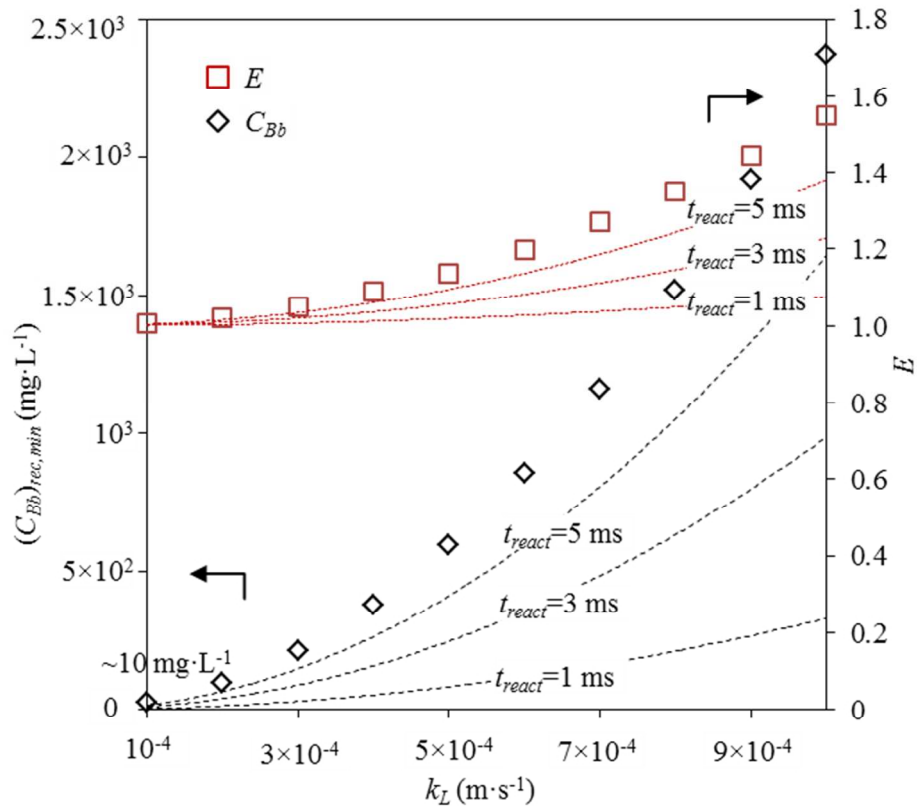


Fig. 12 Variation of the minimum recommended concentration of resazurin $(C_{Bb})_{rec,min}$ and of the corresponding enhancement factor E as a function of the expected magnitude of the liquid side mass transfer coefficient k_L . The term "minimum" means that these parameters are calculated for an Hatta number equal to 3, The dashed curves represent the variations of $(C_{Bb})_{rec,min}$ under various reaction times of the colorimetric reaction, and red dotted curves for E .

82x69mm (300 x 300 DPI)